U. S. Army Ordnance
Ballistic Research Laboratories
Aberdeen Proving Ground, Maryland
Authorization No. 7-4152

EXPLOSIVES RESEARCH CENTER

STRESS WAVES IN BOUNDED MEDIA

Quarterly Report
September 1, 1966 to November 30, 1966

BUREAU OF MINES, PITTSBURGH, PA.

UNITED STATES
DEPARTMENT OF
THE INTERIOR

STRESS WAVES IN BOUNDED MEDIA

Quarterly Report

September 1, 1966 to November 30, 1966

Prepared for:

U. S. Army Ordnance
Ballistic Research Laboratories
Aberdeen Proving Ground, Maryland
Authorization No. 7-4152

by

Richard W. Watson
Karl R. Becker
Frank C. Gibson

Approved:

Robert W. Van Dolah
Research Director
Explosives Research Center

U. S. Department of the Interior
Bureau of Mines
Pittsburgh, Pa.
January 4, 1967

STRESS WAVES IN BOUNDED MEDIA

Introduction

A program to compare the performance of 1.1-inch diameter precision shaped charge assemblies loaded with either a liquid explosive or a solid explosive was completed and is discussed in this report. It was found that the use of the liquid explosive resulted in improved performance at very long standoffs. In addition, studies related to the phenomena of detonation quenching were made, using electronic instrumentation to study the behavior of detonation waves entering a dynamically precompressed region of explosives. A marked difference was observed between the solid and liquid explosives used. Several new methods for increasing energy transfer from detonating explosives were also explored.

Studies with Precision Shaped Charge Assemblies

Penetration and hole-volume data as a function of standoff were accumulated for shaped charges having precision conical liners with base diameters of 1.1 inch. Both a liquid explosive and a solid explosive were used in this investigation in an attempt to determine the effect of charge inhomogeneities on long standoff performance.

The liners were copper cones having a 1.100-inch base diameter, a 42-degree apex angle, and a 27.5-mil wall thickness. The cones were confined in steel charge bodies[1/] which were loaded with either nitroglycerin-ethylene glycol dinitrate (NG-EGDN) liquid explosive, or Composition B solid explosive. A sketch of the charge assembly is shown in figure 1. For initiating purposes, the charge head was fitted with a vented Plexiglas holder for the booster and

1/ The cones and charge bodies were supplied by the Defense Research Division of the Firestone Tire and Rubber Company, Akron, Ohio.

Primacord. The vents were essential for the liquid explosive firings; however, for symmetry, the same holder was also used for the solid explosive charges. The charges were fired into stacks of 4-inch x 4-inch x 1-inch thick steel targets of 4130 steel which was heat treated and oil quenched to a hardness of about 275 BHN.

Penetration data and the corresponding hole-volume data are given in table 1. Firings with NG-EGDN were conducted at seven standoff distances ranging from 2.5 charge diameters (2.75 inches) to 30 charge diameters (33.0 inches); Composition B firings were made at the four longest standoffs. Penetration-standoff curves for the two explosive systems are shown in figure 2. The NG-EGDN firings produced a maximum average penetration of 5.97 inches at 7.5 charge diameters standoff; with increasing standoff, the penetrations steadily declined to a value of 2.03 inches at 30 diameters standoff. Penetrations at 2.5 and 5.0 diameters standoff were only slightly less than the maximum observed. Corresponding Composition B penetrations were 15 to 37 percent less than those observed for NG-EGDN. The variations between trials, for the NG-EGDN penetrations, were larger than anticipated. However, a comparison of the standard deviations shows that the NG-EGDN variations were, in two cases, about equal to, and in the two other cases, considerably less than corresponding variations obtained for Composition B.

The hole-volume data are plotted in figure 3 and indicate a maximum hole volume for the NG-EGDN shots of about 5 cc occurring at the shortest standoff (2.5 charge diameters); thereafter, hole volume decreases monotonically with standoff to a value of about 3 cc at a standoff of 30 charge diameters. Corresponding hole-volume data for Composition B are slightly, but significantly, less (about 4 to 8 percent less) than those observed for NG-EGDN

TABLE 1. - Penetration and hole volume data for 1.1-inch diameter, 42-degree, copper cones fired into steel target material

Standoff (charge diameter)	Penetration (in)	Average Penetration (in)	Hole Volume (cm^3)	Average Hole Volume (cm^3)
		Explosive: NG-EGDN		
2.5	5.68 5.60 5.67	5.65 σ = 0.04	5.01 5.07 4.87	4.98
5.0	5.91 5.38 5.61	5.63 σ = 0.31	4.39 3.97 4.34	4.23
7.5	6.12 5.53 6.27	5.97 σ = 0.43	3.39 4.37 3.86	3.87
10.0	4.62 5.14 4.70 4.80 5.72	5.00 σ = 0.49	3.38 3.71 3.91 4.00 4.16	3.83
15.0	3.71 4.99 4.76 4.00 4.00	4.29 σ = 0.57	3.46 3.90 3.77 3.24 3.71	3.62
20.0	3.15 3.68 3.28 2.95 3.31	3.27 σ = 0.33	3.57 3.54 3.12 3.43 3.45	3.42
30.0	1.91 1.75 2.43	2.03 σ = 0.39	3.01 2.85 3.08	2.98
		Explosive: Composition B		
10.0	3.62 3.68 5.56	4.29 σ = 1.12	3.48 3.76 3.53	3.59
15.0	2.43 3.38 2.75	2.85 σ = 0.55	3.00 3.70 3.46	3.39
20.0	2.32 2.67 2.54 1.33 1.43	2.06 σ = 0.60	3.53 3.30 3.73 2.56 2.68	3.16
30.0	1.62 1.10 1.09	1.27 σ = 0.30	3.03 2.82 2.76	2.87

at the four larger standoffs for which comparisons are available.

Additional investigations using liquid explosive systems are planned and will include tests using precision assemblies with copper liners having a 2.2-inch base diameter.

Detonation Quenching

The results of several different experiments relating to detonation quenching were reported in a recent quarterly report[2/]. Some evidence was given indicating that quenching could occur in dynamically precompressed Composition B; however, the results were inconclusive. More recently, another series of experiments was performed using the arrangement shown in figure 4. The charge geometry was the same as that used in the earlier trials and consisted of a 1/4-inch thick pad of Composition B, precompressed by shock waves derived from a 1/8-inch thick layer of NG-EGDN, and attenuated through 3/8-inch thick Plexiglas plate. To delay pressure release at the bottom surface, the Composition B pad was coupled to a 1/2-inch thick Plexiglas buffer plate. As shown in figure 1, the Composition B was detonated in a direction opposite that of the NG-EGDN; the waves were timed to collide near the center of the charge.

The behavior of the waves prior to and after collision was observed with two resistive pressure gages and six pairs of ionization probes. Figure 5 shows four oscillograms of the gage and probe response, which were obtained in a single firing using four dual-beam oscilloscopes. The time base for all records was 2.0 μsec/major division. The vertical gain for the pressure gage records (fig. 5a) was 2.0 volts/major division while a gain setting

2/ Watson, R. W., K. R. Becker, and F. C. Gibson. Stress Waves in Bounded Media. Bureau of Mines Quarterly Report, U. S. Army Ordnance, Aberdeen Proving Ground, Md., June 1, 1966 to August 31, 1966.

of 5.0 volts/major division was used for the probe records (fig. 5b, c, and d). The upper trace in figure 5a shows the response of gage 1 to the high-velocity detonation in the Composition B pad; the lower trace shows the response of gage 2 to the precompression wave. The pressure delivered to gage 2 was approximately 15 kilobars. The time of arrival of the two waves at the gage stations together with a knowledge of the wave velocities are used to compute the wave collision point relative to the ionization probes. For this particular firing the wave collision occurred 2.5 cm to the left of gage 1 (see fig. 4) or at probe set 2. The upper and lower traces of figure 5b show the response of probe sets 1 and 2 to the detonation wave in Composition B. The peak amplitude of these voltage pulses was approximately 6.0 volts, indicating that the resistance through the ionized detonation products was considerably less than 47 ohms--the value of the load resistance used in the probe circuit. Based on the observation that the wave collision took place near probe set 2, the remaining probe records are interpreted as follows. The initial rise in the upper and lower records of figure 5c corresponds to the arrival of the precompression wave at probe sets 3 and 4, respectively, thus, the precompression wave induces considerable reaction in the Composition B as indicated by the ionization. The sharp subsequent rises in the two records presumably result from the pressure wave associated with the detonating Composition B as it propagates through the precompressed and partially reacted explosive. The average propagation rate of the wave between probe sets 3 and 4 was 4.5 mm/μsec, indicating appreciable deceleration of the wave between probe sets 2 and 3. The remaining two records, corresponding to probe sets 5 and 6, indicate only the partial reaction induced by the precompression wave. Thus, the detonation in the Composition B is effectively quenched approximately 2 cm from the collision point. Under these experimental conditions, quenching occurs in a portion of the explosive that has undergone partial reaction induced by the precompression wave.

The results of similar experiments using a 1/4-inch thick layer of NG-EGDN in place of the Composition B are presented in figure 6. The experimental conditions were the same as in the Composition B firing. The analysis of these records is analogous to that outlined for Composition B. Again, the upper trace in figure 6a shows the response of pressure gage 1 to the detonation wave in the NG-EGDN. The initial pulse on the lower trace corresponds to the precompression wave passing over gage 2 while the second pulse shows the detonation wave in the explosive passing over gage 2 after encountering the precompression wave. Thus, quenching did not occur in the liquid explosive. The wave collision point calculated for this firing was 3 cm to the left of gage 1 or midway between probe sets 2 and 3. The remaining records show the response of probe sets 1 through 6 to the detonation wave in the NG-EGDN. It was noted that there was no indication of any ionization resulting from the precompression wave. The results of these experiments concur with current theories concerning the differences in the initiation mechanisms of solid and liquid explosives.

The ionization phenomenon associated with the precompression wave observed here is deserving of a more detailed study than can be justified by the immediate goals of the stress waves program. For this reason, additional work in this area is being conducted on another program sponsored by BRL.

Composite Explosive Systems

Experiments involving metal plates coupled to composite explosive arrangements were described in two previous reports[3,4/].

3/ Watson, R. W., K. R. Becker, and F. C. Gibson. Stress Waves in Bounded Media. Bureau of Mines Quarterly Report, U. S. Army Ordnance, Aberdeen Proving Ground, Md., March 1 to May 31, 1966.

4/ See work cited in footnote 3.

It was found that, due to a wave shaping mechanism, a higher plate velocity was obtained when the plate was coupled to the explosive component having the lower detonation velocity as opposed to coupling the plate to the high-velocity component. Furthermore, it was noted that this effect was more pronounced as the difference in the detonation velocities of the two explosive components increased. Recent firings were conducted using explosive substances whose detonation velocities were substantially lower than those used previously.

Two low-detonation velocity explosives were each used in combination with Composition B. One of these was a 50-50, by weight, mixture of PETN and common table salt that had a detonation rate of 3.5 mm/μsec; the other was an ammonium nitrate slurry whose basic components were ammonium nitrate, water and aluminum powder with a detonation rate of 3.7 mm/μsec.

One-half inch thick layers of these explosives were coupled to 1/2-inch thick slabs of Composition B. The composite charges were 1-inch thick, 3-inches wide and, 7-1/2-inches or more, long. A typical arrangement is shown in figure 7. The plate material was copper and the plate thickness was adjusted to a C/M ratio of 1.55. Separate firings were conducted with the plates coupled to each explosive component; two trials were made for each configuration.

The data from these firings and other pertinent details concerning the low-rate explosives are given in table 2. The composite charge of Composition B with the slurry gave a plate velocity of 1.44 mm/μsec when the plate was coupled to the slurry and 1.32 mm/μsec, for the reverse configuration, a gain in velocity of about 9 percent.

The detonation velocity of the slurry is about one-half that for Composition B (3.70 mm/μsec vs 7.82 mm/μsec). Since this represents

TABLE 2. - Data from firings for flat plates coupled to composite explosives

Configuration	Plate Thickness (in)	Departure Angle (deg)	Spread (deg)	V_n (mm/μsec)
PETN-salt → Composition B → plate	0.095	10.4	0.0	1.41
Composition B → PETN-salt → plate	0.095	10.4	0.7	1.41
Slurry → Composition B → plate	0.102	9.7	0.5	1.32
Composition B → slurry → plate	0.102	10.6	0.2	1.44

V_n = normal component of plate velocity.

C/M = charge mass/plate mass = 1.55 throughout all firings.

PETN-salt - a 50% by 50% mixture of the explosive substance PETN and finely ground table salt with a mixture density of 0.91 g/cm^3 (granular composition).

Slurry - semi-liquid composition having a density of 1.02 g/cm^3.

NH_4NO_3 - 60%

H_2O - 28.7%

al powder - 10.0%

guar gum - 1.0%

buffer - 0.3%

the largest difference in detonation velocity of any of the composite arrangements to date, one might expect the more pronounced wave shaping to produce the largest gain. This is, however, not the case because previous firings[5/] with nitromethane (NM) (U_D = 6.33 mm/μsec) in a composite arrangement with Composition B produced a gain of about 14 percent with the low-velocity component coupled to the plate. This apparent disparity can be explained in terms of the relative energetics of the explosives used. Previous flat plate and cylinder-type energy coupling experiments with NM and current tests with slurries indicate a significantly higher energy transfer for NM. Thus, both a wave shaping effect and an energetics effect must be considered when comparing the results of different composite explosive arrangements. Lowering the energetics of the explosive used in combinations with Composition B ultimately reduces the effectiveness of the composite arrangement.

The Composition B and PETN-salt charges failed to produce any gain in plate velocity even though radiographs of the wave structure show a marked wave shaping effect. The relative energetics of this explosive mixture has subsequently been found to be quite low. On the basis of tests conducted in copper cylinders, the energy per unit explosive mass was only about one-sixth that obtained for Composition B.

Multi-element Plate Systems

Additional three-element plate work, similar to that previously reported[6/], was performed in which the composite plate arrangement was polyethylene sandwiched between two aluminum plates; however, the current system uses polyethylene with copper as the metallic element. One of the copper elements was about five times

5/ See work cited in footnote 3.
6/ See work cited in footnote 2.

the thickness of the other and the explosive was Composition B. Details of the charge and plate assembly are given in figure 8. The C/M ratio was 1.55; however, it should be pointed out that the scale size of the three-element plate system was about 50 percent greater than the scale size used in other multi-plate systems. The scale size was increased to give a practical thickness to the thin metal element. The results of the firings are given in table 3.

TABLE 3. - Additional results with multi-element plates

Configuration	Outer Plate Departure Angle (deg)	Plate Velocity (mm/μsec)
Composition B coupled to thick copper plate	11.2	1.52
Composition B coupled to thin copper plate	9.6	1.30

The departure angles given are averages of two trials; variations were small. The significant result is that the thin copper plate attained a velocity of 1.52 mm/μsec with the explosive coupled to the thick copper plate, compared to a velocity of 1.30 mm/μsec for the thick copper plate in the reverse configuration. This result is consistent with that obtained for the three-element plate system using aluminum plates; both these systems showed a 17 percent gain in plate velocity.

For reference and comparison purposes, all the multi-element plate tests to date, including pertinent single-element plate firings, are compiled in table 4.

Colliding Plate Experiments

Another possible method for increasing plate velocities that

TABLE 4. - Summary of multi-element plate experiments

Configuration	Plate Velocity
I. Single-element Plates	
(1) Composition B (1") → cu (.125)	1.49
(2) Composition B (1") → al (.412)	1.45
(3) Composition B (1") → mg (.639)	1.43
II. Two-element Plates (metal-metal type)	
(1) Composition B (1") → mg (.320) → cu (.062)	1.51 (cu plate)
(2) Composition B (1") → cu (.062) → mg (.320)	1.51 (mg plate)
III. Two-element Plates (metal-plastic type)	
(1) Composition B (1") → plastic (.125) → cu (.112)	1.55 (cu plate)
(2) Composition B (1") → cu (.112) → plastic (.125)	1.77 (plastic plate)
(3) Composition B (1") → plastic (.125) → al (.369)	1.49 (al plate)
(4) Composition B (1") → al (.369) → plastic (.125)	1.77 (plastic plate)
IV. Three-element Plates (metal-plastic metal type)	
(1) Composition B (1.5") → al (.062) → plastic (.125) → al (.306)	1.51 (.306 al plate)
(2) Composition B (1.5") → al (.306) → plastic (.125) → al (.062)	1.77 (.062 al plate)
(3) Composition B (1.5") → cu (.031) → plastic (.125) → cu (.143)	1.30 (.143 cu plate)
(4) Composition B (1.5") → cu (.143) → plastic (.125) → cu (.031)	1.52 (.031 cu plate)

C/M = 1.55 for all configurations.

Plate velocities given are for the "outer" plate, i.e., the plate with a free surface.

Numbers in parentheses are plate thicknesses in inches.

was explored during this report period is illustrated in figure 9. In this case an explosive-loaded plate was driven across a 1/2-inch air gap into a stationary plate. The principle here is best envisioned in terms of simple collision theory. For a perfectly elastic collision and small impact angles, the impacted plate could attain a velocity approaching twice that of the explosively driven plate.

The radiographs from two such experiments are presented in figure 10. The upper radiograph shows a light-weight plate colliding with a heavier plate with a subsequent decrease in velocity. The lower radiograph shows the reverse situation with a gain in velocity. The data from a number of plate collision trials involving copper and aluminum plates having different plate mass ratios and different collision velocities are presented in table 5. As noted, the velocities of the explosive-driven plate after the collision are presented for certain cases where the plate profile was clearly discernible in the radiographs. The highest plate velocity ratio observed was 1.21 with a corresponding plate mass ratio of 6.37. This is considerably lower than estimates calculated from simple collision theory assuming perfectly elastic behavior, indicating that considerable energy is dissipated in the collision process. This method of increasing plate velocity shows some promise but further experiments will be delayed until other approaches have been explored.

TABLE 5. - Summary of colliding plate experiments

$\frac{M_1}{M_2}$	V_1	V_2	V_1'	$\frac{V_2}{V_1}$	$\frac{V_1'}{V_1}$
		Copper → Aluminum			
6.37	1.49	1.81	1.34	1.21	0.90
3.19	1.83	2.16	1.63	1.18	0.98
3.19	1.49	1.77	1.30	1.18	0.87
1.60	1.49	1.65	0.61	1.11	0.41
1.00	2.34	1.70	-	0.73	-
		Aluminum → Copper			
1.25	1.64	1.73	0.94	1.05	0.57
0.312	2.91	1.56	-	0.536	-

$\frac{M_1}{M_2}$ = mass ratio of explosively driven plate to collided plate.

V_1 = initial velocity of explosively driven plate.

V_1' = final velocity of explosively driven plate.

V_2 = final velocity of collided plate.

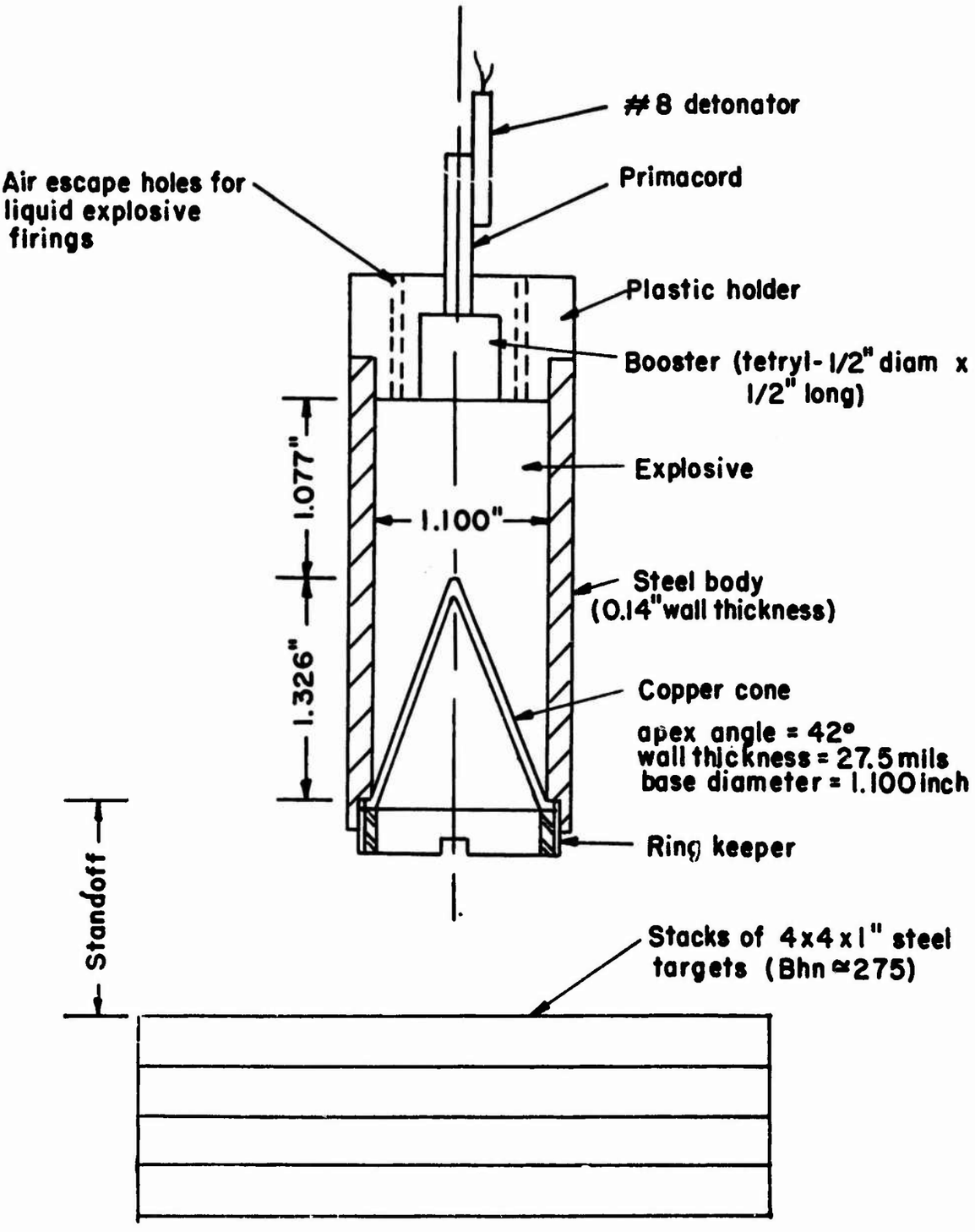

FIGURE 1. - Sketch of charge assembly used in precision cone firings.

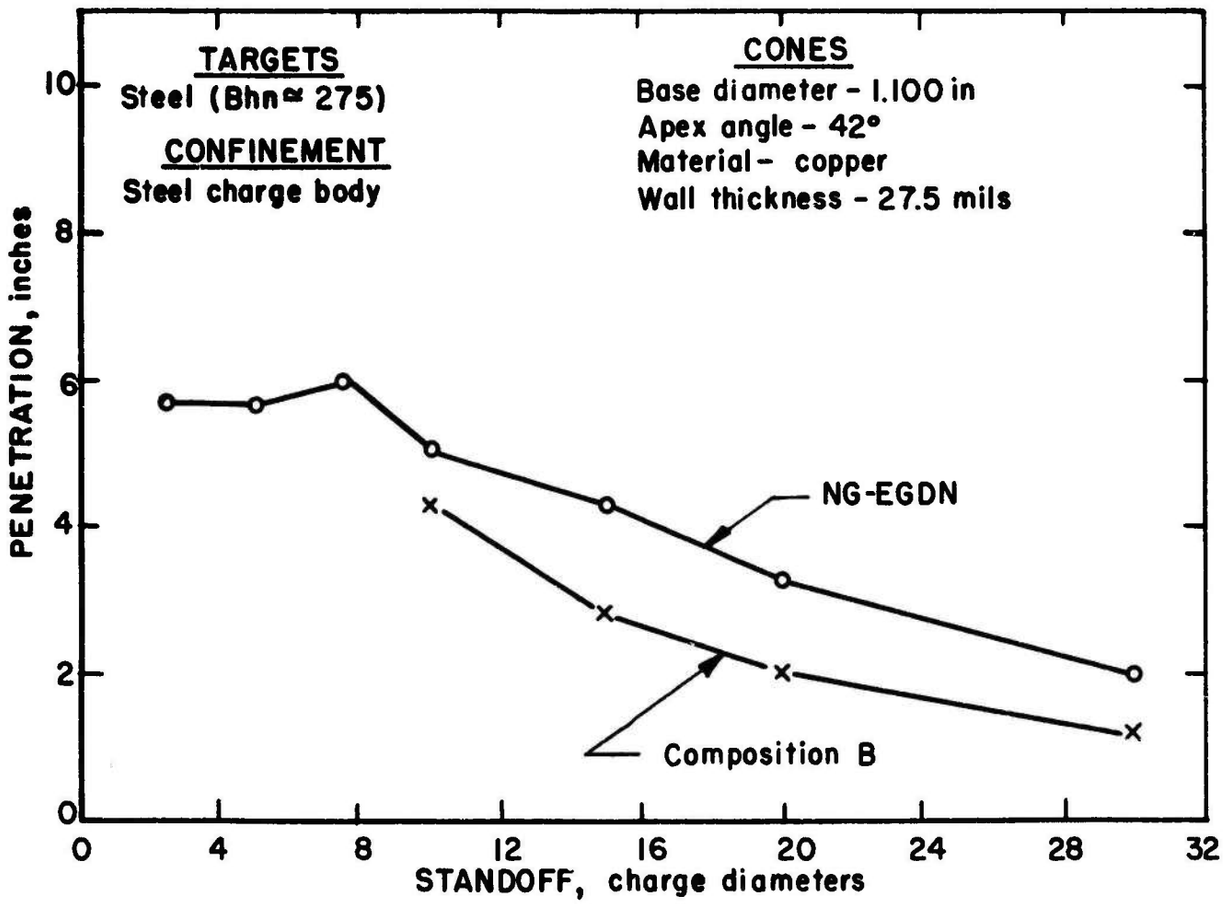

FIGURE 2. - Penetration versus standoff for precision shaped charges fired into steel targets.

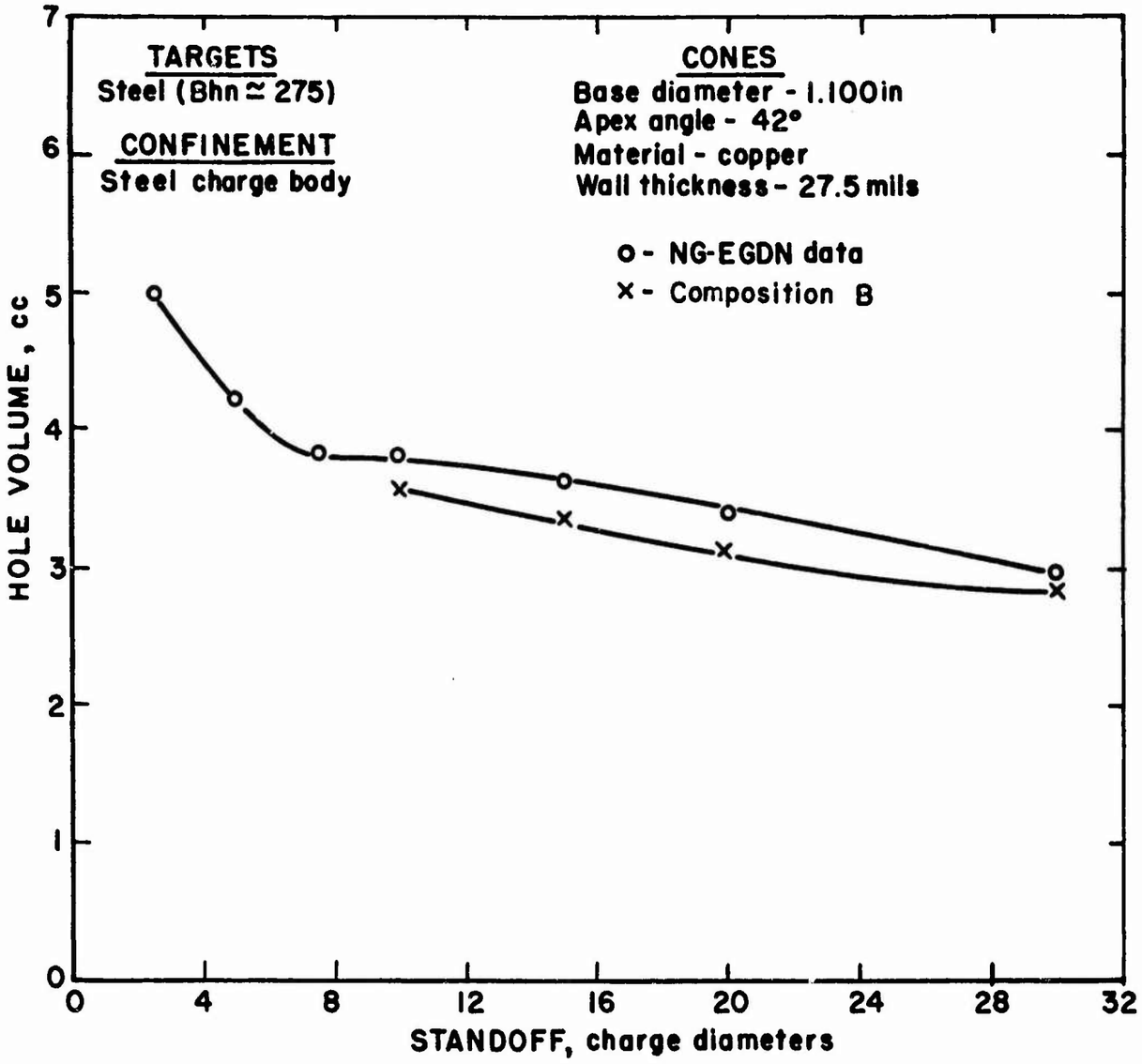

FIGURE 3. - Hole volume versus standoff for precision shaped charges fired into steel targets.

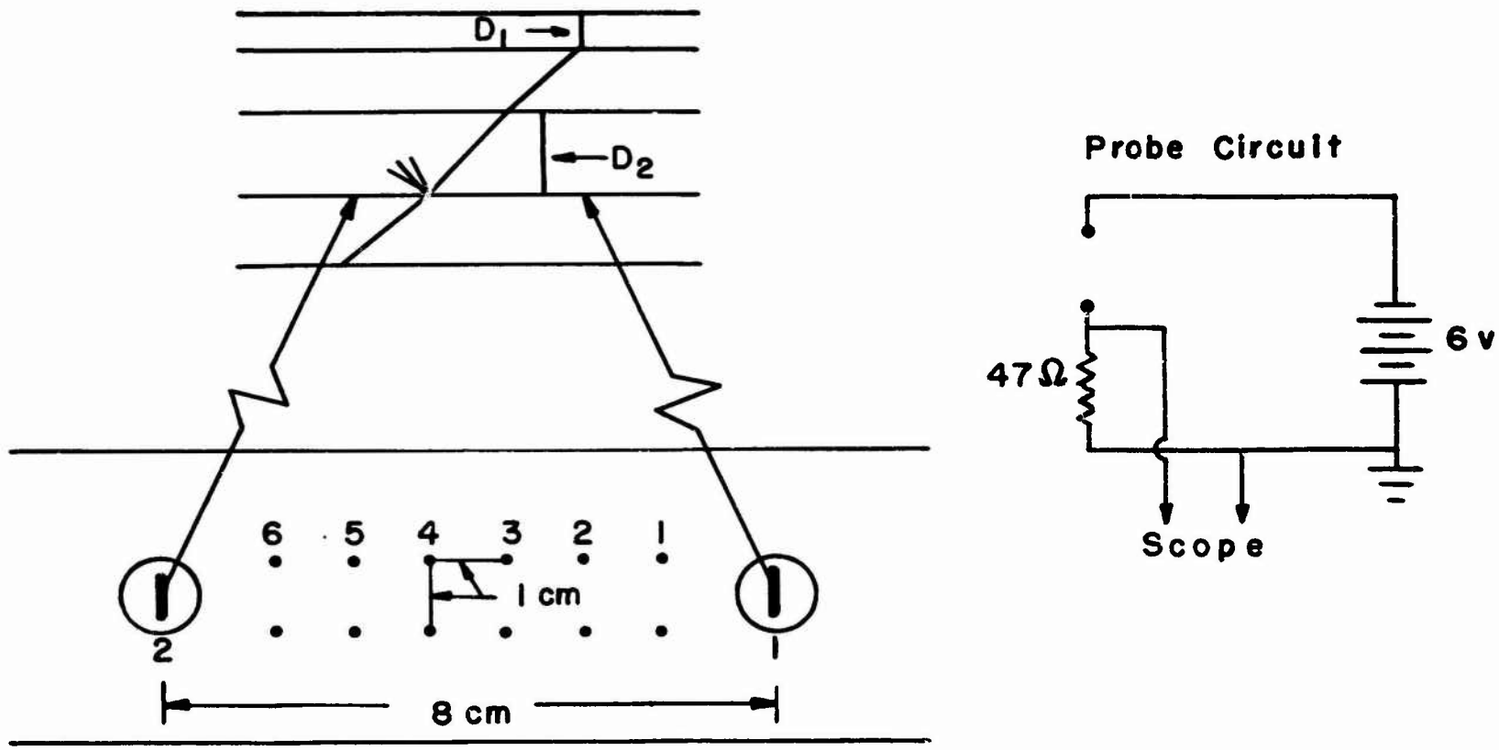

FIGURE 4. - Experimental arrangement used to study the detonation quenching.

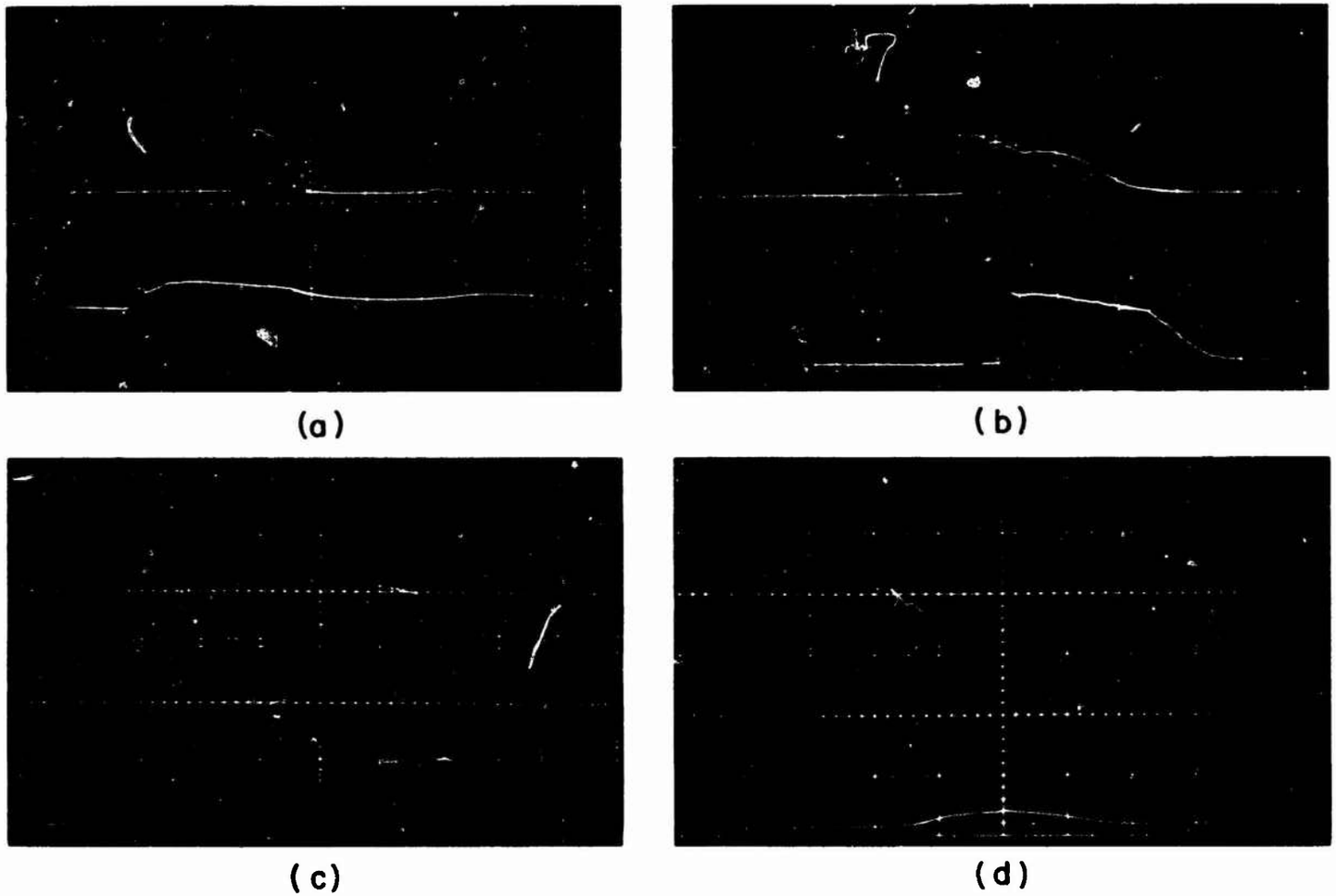

FIGURE 5. - Oscillograms for a quenching experiment using Composition B.

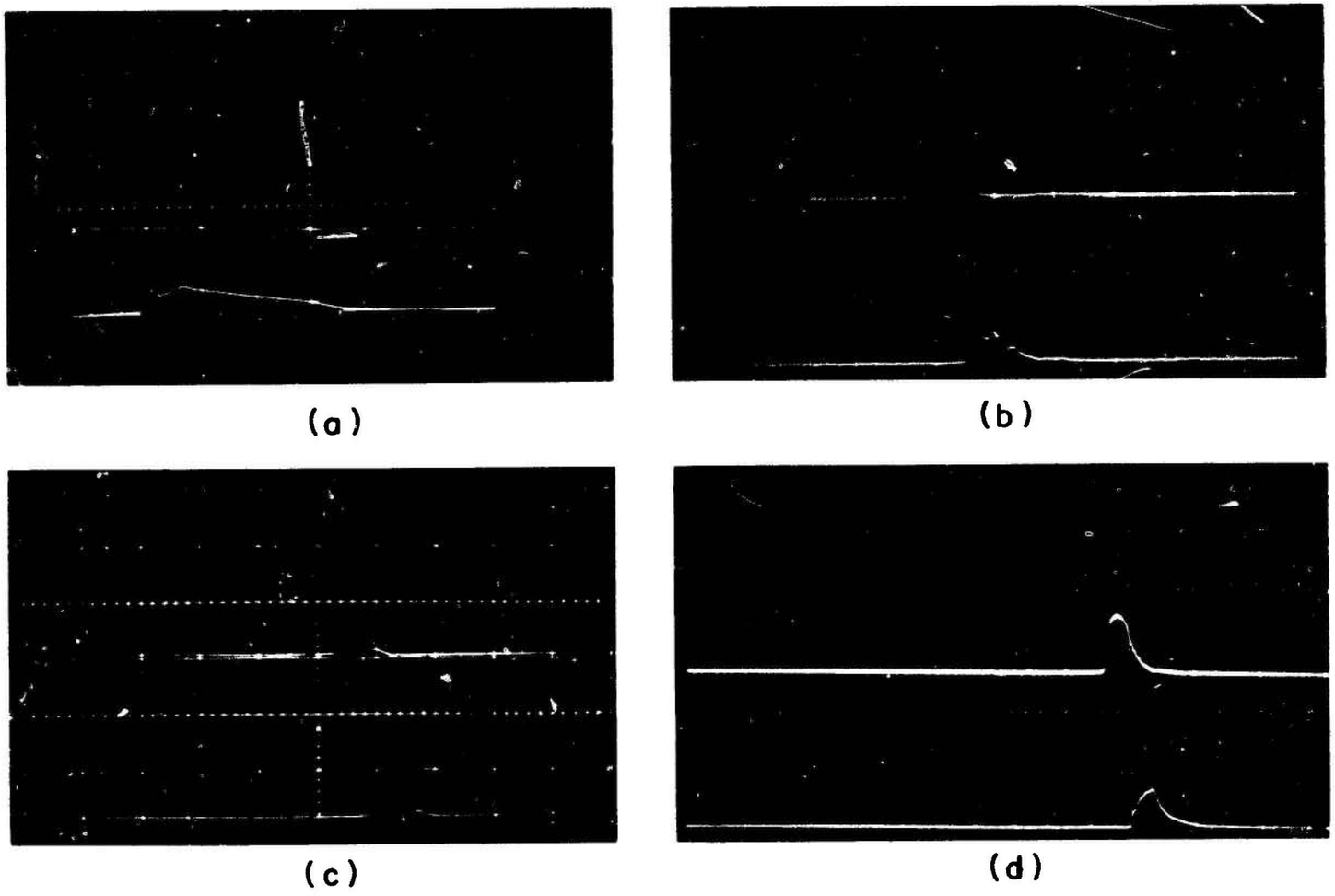

FIGURE 6. - Oscillograms from a quenching experiment using NG-EGDN.

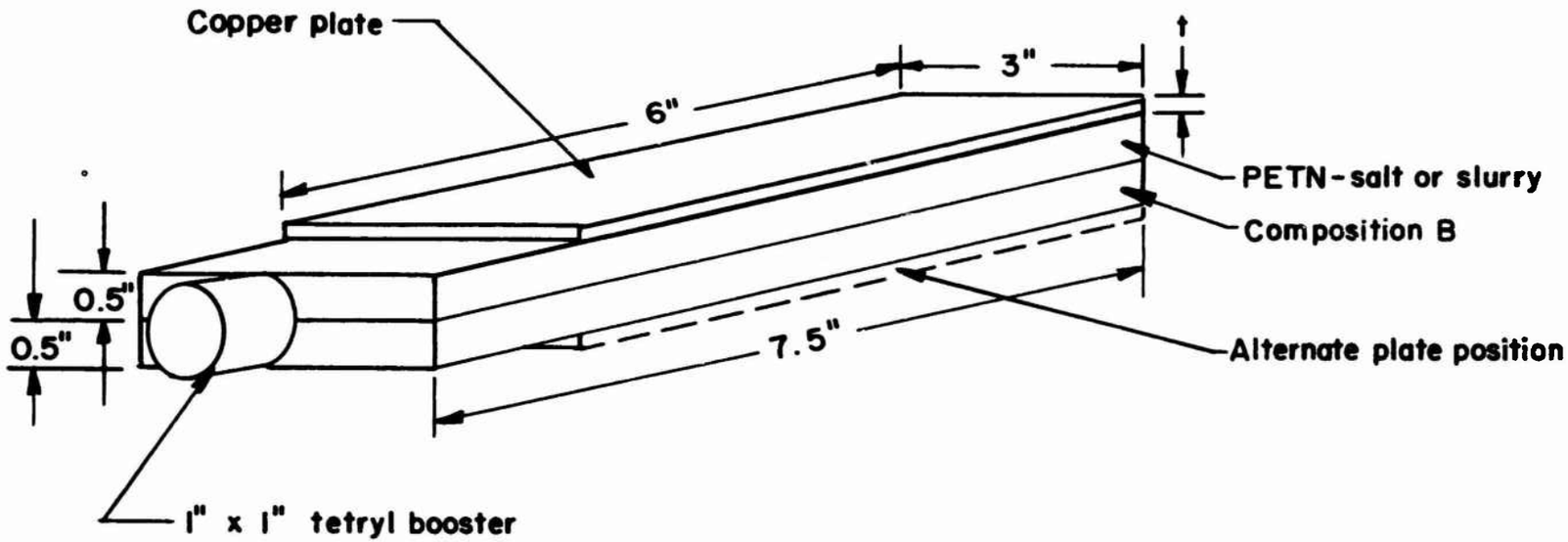

FIGURE 7. - Sketch of composite explosive-plate assembly.

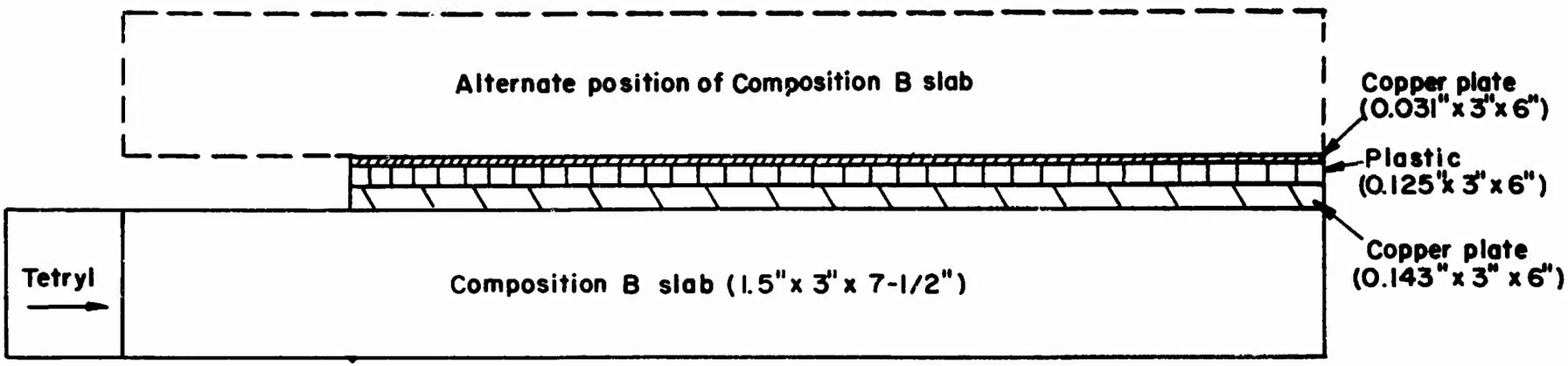

FIGURE 8. - Sketch of tri-element plate and explosive assembly.

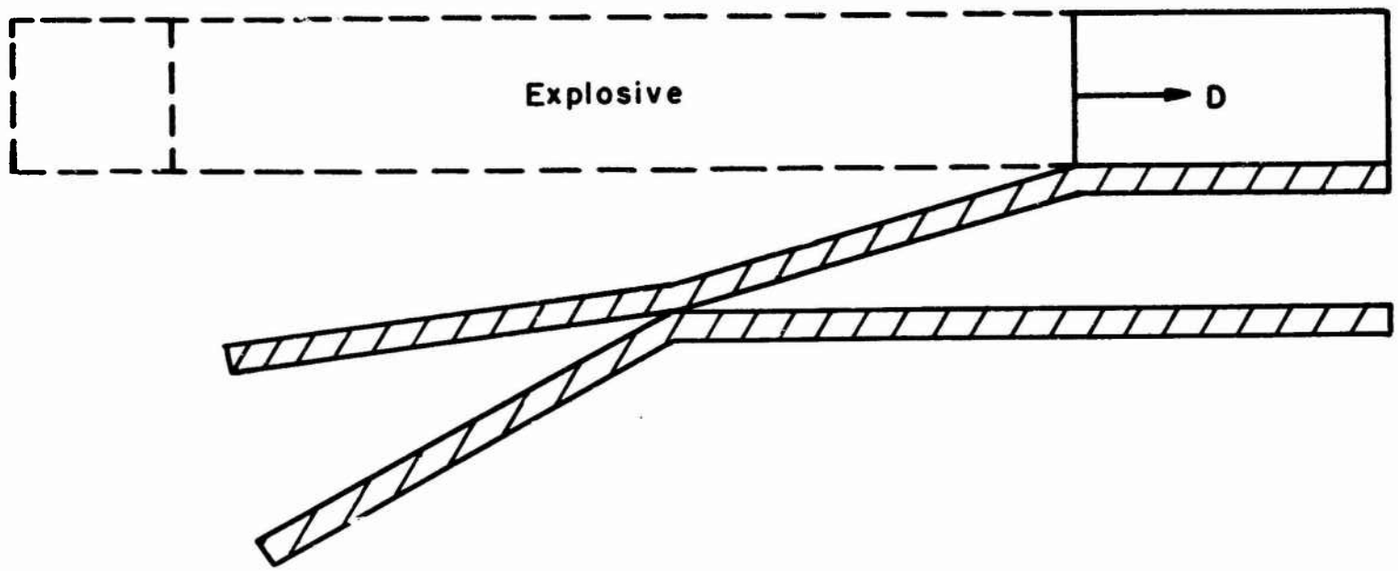

FIGURE 9. - Sketch of colliding plate firing.

0.653-IN COMPOSITION B + 1/16-IN ALUMINUM ⟶ 1/16-IN COPPER

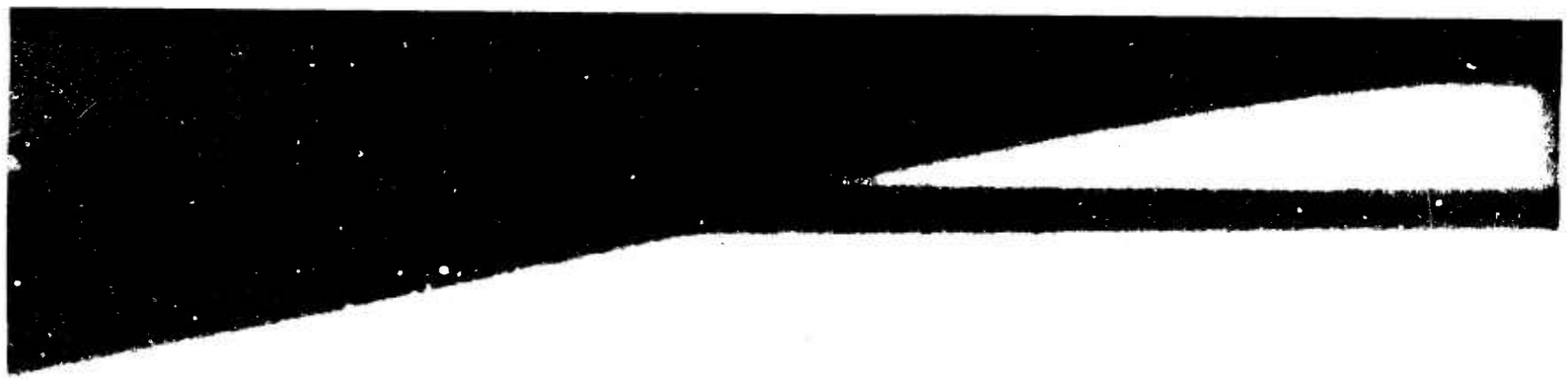

1.0-IN COMPOSITION B + 1/8-IN COPPER ⟶ 1/8-IN ALUMINUM

FIGURE 10. - Radiographs from two colliding plate trials.